6. A. Dar and G. Shaviv, Technion Preprint, Technion-Ph-94-5 (1994).
7. A. M. Mukhamedzhanov and N. K. Timofeyuk, *Pisma Zh. Eksp. Teor. Fiz.* **51**, 247 (1990).
8. R. B. Kavanagh *et al.*, *Bull. Am. Phys. Soc.* **14**, 1209 (1969).
9. B. W. Filippone *et al.*, *Phys. Rev. Lett.* **50**, 412 (1983); *Phys. Rev. C* **28**, 2222 (1983).
10. C. W. Johnson *et al.*, *Astrophys. J.* **392**, 320 (1992).
11. T. Motobayashi *et al.*, RIKEN Preprint RIKKYO RUP-92-2 (1994).
12. J. N. Bahcall, *Phys. Rev.* **128**, 1297 (1962).
13. V. Castellani *et al.*, *Astron. Astrophys.* **271**, 601 (1993).
14. W. A. Fowler, *Nature* **238**, 24 (1972).
15. V. Castellani *et al.*, Instituto Nationale Fizica Nucleare (INFN)–Ferrara Preprint INFNFE-3-94 (1994).
16. K. Hirata *et al.*, *Phys. Rev. Lett.* **65**, 1301 (1990); *Phys. Rev. D* **44**, 2241 (1991).
17. B. Pontecorvo, *Atomic Energy of Canada Limited Chalk River Lab. Rep. PD-205* (1946).
18. L. W. Alvarez, *Univ. Calif. Radiat. Lab. Rep. UCRL-328* (1949).
19. P. Anselmann *et al.*, *Phys. Lett. B* **327**, 377 (1994).
20. J. N. Abdurashitov *et al.*, *Los Alamos Rep. LA-UR 94-1113* (1994); *Phys. Lett.*, in press.
21. D. R. O. Morrison, in Proceedings of the 25th International Conference on High Energy Physics, Singapore, K. K. Phua and Y. Yamaguchi, Eds. (World Scientific, Singapore 1991), p. 676.
22. S. Pakvasa, in (*21*), p. 698; J. N. Bahcall and H. A. Bethe, *Phys. Rev. D* **47**, 1298 (1993); M. Spiro and D. Vigneaud, *Phys. Lett. B* **242**, 279 (1990).
23. N. Hata *et al.*, *Phys. Rev. D* **49**, 3622 (1994).
24. W. Kwong and S. P. Rosen, *Phys. Rev. Lett.* **73**, 369 (1994).
25. J. N. Bahcall, Institute of Advanced Study Preprint IASSNS-AST 94/37 (1994).
26. ——, *Phys. Rev. D* **44**, 1644 (1991).
27. B. Pontecorvo, *Zh. Eksp. Teor. Fiz.* **53**, 1717 (1967); M. Nakagawa *et al.*, *Prog. Theor. Phys.* **30**, 727 (1963).
28. S. Glashow and L. Krauss, *Phys. Lett. B* **190**, 197 (1987); S. Bilenky and B. Pontecorvo, *Phys. Rep.* **41**, 225 (1978); V. Barger *et al.*, *Phys. Rev. D* **24**, 138 (1981).
29. S. P. Mikheyev and A. Smirnov, *Nuovo Cimento* **19**, 17 (1986).
30. L. Wolfenstein, *Phys. Rev. D* **20**, 2634 (1979).
31. P. Krastev and S. Petcov, *Phys. Rev. Lett.* **72**, 1960 (1994).
32. N. Hata, *Univ. Penn. Rep. UPR-0605-T* (1994).
33. —— and P. Langacker, *Univ. Penn. Rep. UPR-0592T* (1993).
34. R. S. Raghavan, in (*21*), p. 482.
35. G. Bellini *et al.*, Eds., "Borexino at Gran Sasso: A Real-Time Detector for Low Energy Solar Neutrinos" (INFN-Milan Report, 1991).
36. "Borexino Progress Report" (INFN-Milan Report, 1993).
37. Y. Totsuka, *Univ. of Tokyo (ICRR) Rep. ICRR-227-90-20* (1990).
38. G. T. Ewan *et al.*, Sudbury Neutrino Observatory Proposal *SNO-87-12* (1987).
39. H. Chen, *Phys. Rev. Lett.* **55**, 1534 (1985).
40. N. Hata, in (*1*).
41. S. Pakvasa and J. Pantaleone, *Phys. Rev. Lett.* **65**, 2479 (1990).
42. R. S. Raghavan *et al.*, *ibid.* **71**, 4295 (1993).
43. R. Lanou *et al.*, *ibid.* **58**, 2498 (1987).
44. T. Ypsilantis, in Proceedings of the II Nestor International Workshop, Univ. of Athens, Pylos, Greece, October 1993, K. Resvanis, Ed., in press.
45. E. Fiorini and T. Niniikoski, *Nucl. Instrum. Methods* **224**, 83 (1984).
46. P. F. Smith *et al.*, *Phys. Lett. B* **245**, 265 (1990).
47. I wish to thank J. Pantaleone and P. Raghavan for generous help with theoretical calculations, N. Hata for Figs. 2 and 5, and S. Pakvasa for long-standing discussions.

High-Luminosity Blue and Blue-Green Gallium Nitride Light-Emitting Diodes

H. Morkoc and S. N. Mohammad

Compact and efficient sources of blue light for full color display applications and lighting eluded and tantalized researchers for many years. Semiconductor light sources are attractive owing to their reliability and amenability to mass manufacture. However, large band gaps are required to achieve blue color. A class of compound semiconductors formed by metal nitrides, GaN and its allied compounds AlGaN and InGaN, exhibits properties well suited for not only blue and blue-green emitters, but also for ultraviolet emitters and detectors. What thwarted engineers and scientists from fabricating useful devices from these materials in the past was the poor quality of material and lack of *p*-type doping. Both of these obstacles have recently been overcome to the point where high-luminosity blue and blue-green light-emitting diodes are now available in the marketplace.

While semiconductor coherent light sources, or lasers, continue to lure scientists and engineers, their cousins, light-emitting diodes (LEDs), have improved remarkably in terms of both brightness and the range of wavelengths of emission available (*1*). Early LEDs were limited to red light and luminous fluxes (*2*) of about 0.1 to 0.2 lm/W, which restricted their application. Over the years, red, orange, amber, and green emitters have been made with considerable enhancements in performance. With the recent introduction of blue LEDs, these emitters now span the entire range of visible wavelengths with luminous flux sufficiently high to pave the way even for outdoor LED displays and lighting.

The authors are at the University of Illinois at Urbana-Champaign, Materials Research Laboratory and Coordinated Science Laboratory, Urbana, IL 61801, USA.

Current LEDs are very reliable and have many applications. These ubiquitous devices will continue to expand their applications in displays, lighting, indicator lights, advertisement, traffic signs and traffic signals, light sources for accelerated photosynthesis, and medicine for diagnosis and treatment (*3, 4*). As light sources, LEDs are likely to be more efficient and reliable than incandescent lighting. In addition, white light illumination (*5*) by means of primary color addition is simple and has the advantage of achieving any desired color tone in the chromaticity diagram by appropriately mixing those colors in a light scrambling configuration. This requires bright green and blue sources in addition to the bright red LEDs that are already available. Made from commercially available LEDs, a display chip made in Japan uses six SiC blue, four GaP green, two AlGaAs amber, and two AlGaAs red LEDs (*6*). With the recently introduced bright blue GaN-based LEDs, the number of blue devices needed can be reduced. If used in place of incandescent light bulbs, these LEDs would consume only about 10 to 20% of the power for the same luminous flux with the added advantage of compactness and much longer lifetime, 2000 hours for the former as opposed to tens of thousands for the latter.

Traffic lights at present rely on filtration of incandescent light to achieve a particular color, which is an energy-inefficient technique. Moreover, they require large repair crews for maintenance. With recently introduced blue-green 500-nm LEDs, the traffic lights can be replaced with efficient LEDs that have superior longevity. Along similar lines, the high mounted brake lights in recent model automobiles and running lights in trucks make use of red AlGaAs LEDs. It is expected that other colors will follow.

Light Emission from Diodes

LEDs are very efficient converters of electricity to light. This phenomenon results from the intrinsic or inherent properties of the semiconductors from which they are made. Semiconductors represent an important class of materials characterized by two energy bands: the valence band and the conduction band. In an intrinsic semiconductor under normal conditions, the valence band is filled with a large number of electrons, whereas the conduction band, lying at a higher energy, is practically empty. Electrical conductivity is attributable to the transport of electrons in the conduction band and can be changed by filling the conduction band with electrons donated by appropriate impurity atoms. The electrons populating the conduction band are not only mobile but also make the transition across the band gap to the valence band. In direct–band gap semiconductors, where the valence band and conduction band minima occur for the same (typically zero) momentum value, this transition is radiative, meaning it results in the emission of photons. When an injected electron recombines with a hole in the valence band without the involvement of defect states, an electron-hole recombination takes place, and the loss of energy of the electron appears as photons (Fig. 1) (*7*). The energy of the photon is approximately equal to the energy difference E_g across the band gap at the point where recombination occurs, unless impurity transitions are involved, which is the case for InGaN. The most favorable situation under which a radiative recombination takes place is at zero momentum for both electrons and holes. Depending on E_g, different wavelengths of the radiative photons result. The LED devices are optimized for this emission.

A laser diode represents an extension of the LED and incorporates a region of light guide. This light guide contains a region where photons multiply and optical gain is provided. A feedback system converts the photon amplifier into an optical oscillator. Being more complex than an LED, it needs to satisfy a few more optical and design criteria as well.

Detection and measurement of radiant electromagnetic energy is called radiometry, which when applied to the visible portion of the spectrum involving the human eye is termed photometry (*8, 9*). The nomenclature for the latter delineates itself from the former by adding the adjective luminous to the terms used for the former. For example, energy in the former is called the luminous energy in the latter. Values can be converted between the two if the perception of color by the human eye, eye response, is known. In daylight, the human eye is most sensitive to light with a wavelength of 555 nm with a maximum sensitivity of 683 lm/W. This is called the photopic vision. In low light and night situations, the peak sensitivity blueshifts to 507 nm. This is classified as the scotopic vision. The maximum sensitivity for the scotopic vision is 1754 lm/W. At the red and blue extremes, the sensitivity of the human eye drops dramatically. Consequently, light sources near these extremes must be very efficient emitters to be practical.

Structure and Synthesis

An LED, in its simplest form, is produced by growing an *n*-type material on a *p*-type base, or vice versa. An *n*-type material is realized by doping an intrinsic material with donor atoms, and a *p*-type material by doping it with acceptor atoms. Donors are elements that have one or more valence charge than the host, whereas acceptors have one less valence charge than the host. Thus, an *n*-type region has an excess of electrons, and a *p*-type region an excess of holes. Forward biasing results in an increase in the number of electrons on the *p* side and of holes on the *n* side, thus providing an increased probability of radiative recombination of electron-hole pairs. The region that has an abundance of both types of carriers can be limited to a small volume by flanking both sides of that region with a semiconductor with a large band gap. Such recombinations are responsible for light emission in LEDs.

In order to develop bright LEDs with desired colors, the manufacturer must fabricate them from semiconductors of very high quality. During the past few years, III-V nitride films have been grown from the vapor phase by several well-known techniques such as high-pressure (*10*) and low-pressure (*11*) chemical vapor deposition (CVD) and plasma-enhanced molecular beam epitaxy (MBE) (*12*). In one high-pressure growth technique, Ga metal or GaN powder sublimed at high temperature under a significant N_2 or NH_3 overpressure is transported to a reaction zone to grow single-crystal III-V nitride films, unfortunately with marginal success. For substrates, the ubiquitous substrate material sapphire was used, which is not very well lattice-matched to III-V nitrides; lattice parameters and coefficients of thermal expansion for sapphire are respectively about 23% and 25% higher than the corresponding figures for GaN (a = 3.189 Å). Yet this transparent material found wide application as substrates in the growth of nitride films. Alternative substrates—including silicon carbide (SiC, a = 3.08 Å, lattice mismatch of about 4%), magnesium oxide (MgO, a = 4.216 Å), and zinc oxide (ZnO, a = 3.252 Å, lattice mismatch of about 2%)—have been explored. Silicon carbide is now available commercially and is under consideration for use in lieu of sapphire, which is currently used in commercial InGaN LED production.

Commercial InGaN LEDs have been produced with a variant of the CVD technique known as metal organic chemical vapor deposition (MOVPE) (*11, 13*). Organic chemicals such as trimethylgallium, trimethylaluminum, and trimethylindium are allowed to react with ammonia at a substrate temperature of roughly 1000°C. In improved versions of MOVPE reactors, reactant gases diluted with H_2 enter the growth area through a quartz nozzle that directs the flow down onto the rotating substrate. Ammonia is directed downward on the heated substrate for efficient decomposition and reaction. This so-called vertical design is credited with the improvement

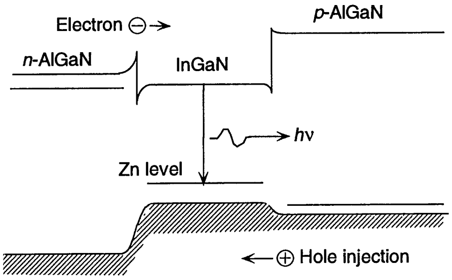

Fig. 1. Conduction and valence band edges of a *pn* double heterojunction InGaN-AlGaN LED under injecting conditions.

of the interaction of the reactant gases with the substrate stemming from a downward flow of H_2 and N_2. The MOVPE process is inherently very complex to understand. To this end, the MBE technique, which is simpler, is gaining considerable interest for comprehensive investigations and the production of novel structures.

Control of the III-V nitride electrical properties, particularly the electrical conductivity, has traditionally been, and still is, one of the greatest challenges facing III-V nitride researchers. In general, good conductivity results when an *n*-type semiconductor's donor levels lie close to the conduction band edge or a *p*-type semiconductor's acceptor levels lie close to the valence band edge. Thus, lying in "shallow" levels, the dopant atoms are easily ionized at device operating temperatures, creating free carriers in the respective bands. Unintentionally doped (a term used to describe semiconductors that naturally contain defects in addition to those introduced by doping) GaN and InN suffer from *n*-type background carrier concentrations, except in films of poor quality, which are compensated by deep levels. With improved crystal growth techniques, researchers in several laboratories have succeeded in reducing the background electron concentration *n* to as low as 10^{16} cm^{-3}. Nakamura *et al.* (*14*) have reported GaN bulk mobility of μ_n = 600 and 1500 $cm^2 V^{-1} s^{-1}$ at 300 and 77 K, respectively, in an undoped sample having $n = 4 \times 10^{16}$ cm^{-3}. The lower the background concentration, the better the chances for the semiconductor to obtain *n* or *p* type. Moreover, the properties of the semiconductor can be analyzed with better sensitivity now that the camouflaging effects of unintentional doping are no longer present. The InN films have proved more difficult to grow and usually have background electron concentrations well in excess of 10^{18} cm^{-3}. Generally, AlN is observed to be insulating, although recent Ge-doped samples show electrical conduction; this is attributed to its donor, acceptor, and defect levels lying deep within the band gap.

Successful *p* doping has been the major

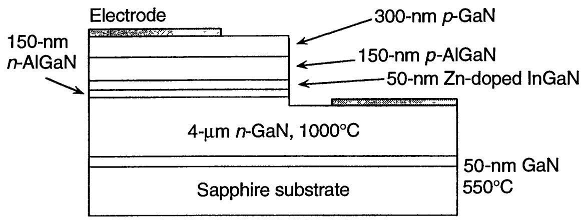

Fig. 2. A schematic cross-sectional view of the Nichia InGaN-AlGaN-GaN double heterojunction LED on sapphire. The insulating nature of the substrate necessitates surface electrodes, and the light can be collected from the top or the bottom because the substrate is transparent to the wavelength of emission.

catalyst in the resurgent interest in the nitrides. Until recently, efforts to dope GaN to convert it to *p* type have led to compensated high-resistivity material. In fact, in the original metal-insulator LEDs developed in the early 1970s by Pankove *et al.* (*15*), then at RCA Laboratories, a high-resistivity region was used as host for recombination with ensuing photon emission. An observation that compensated Mg-doped GaN could be converted into conductive *p*-type material by low-energy electron beam irradiation (LEEBI) (*16*) marked a breakthrough, which led Nakamura *et al.* (*17*) to use LEEBI to achieve GaN with $p = 3 \times 10^{18}$ cm^{-3} and a resistivity of 0.2 ohm·cm. It was thereafter discovered that thermal annealing at 700°C under an N_2 ambient converted the material to *p* type equally well. The process was observed to be reversible, with the GaN reverting to insulating compensated material when annealed under NH_3. Hydrogen was thus identified as the critical compensating agent. Workers in several laboratories have used hydrogen-free growth techniques, notably electron cyclotron resonance (ECR)–based MBE, to achieve *p*-type conductivity in as-grown wurtzite and zincblende GaN (*12*). Because the binding energy of Mg is not as close to 500 MeV as it is for Cd and Zn, acceptor activation ratios of only 10^{-2} to 10^{-3} are typically achieved. Therefore, very large amounts of Mg must be incorporated to obtain high doping levels. Van Vechten *et al.* (*18*) have proposed a plausible model describing H acceptor compensation in GaN in which Mg-H defect complexes are converted to conventional acceptor impurities by annealing or LEEBI. With the realization (*16*) of *p*-type GaN by LEEBI, the fabrication of the *pn*-junction GaN LED was possible for the first time. Soon after, AlGaN was introduced as a barrier material (*19*) to block the escape of injected minority carriers (Fig. 1), which was used by Nichia Chemical Industries and Toyota Gosei to develop impressive GaN-based LEDs.

In an effort to realize reduced substrate temperatures and a hydrogen-free process, many groups have turned to MBE, where reactive N species are supplied from ammonia gas or N_2 predominantly by an ECR source. Other energetic sources that impart kinetic energy to nitrogen molecules—such as supersonic jet sources with and without radio frequency (RF) augmentation, RF sources, and mass-selective sources with neutralizers—are being considered. The reduced temperatures and greater flexibility of MBE have allowed many other substrate materials to be investigated, including GaAs, MgO, and ZnO. Researchers have also demonstrated that *p*-type Mg-doped GaN can be grown directly with MBE without the need for post-growth processing, as a result of the H-free growth environment (*20*).

Performance of LEDs

The injection of electrons on the *p* side of an LED and holes on the *n* side, accomplished by forward biasing, increases the probability of radiative recombination. If all of the injected electrons recombined and if all the recombinations were radiative, the internal quantum efficiency of the LED would be 100%. Unfortunately, nonradiative recombinations, which usually occur at lattice imperfections of the crystals, and light absorbed and trapped in the semiconductor after emission lower the effective efficiency, which is called the external efficiency. The latter is taken care of in a laser diode as the light is guided and coupled out of the semiconductor. Additional loss of power occurs in converting electricity to optical power, such as loss across parasitic resistances.

Appropriate engineering techniques are used to increase the efficiency, which involves the use of heterojunctions so that self-absorption of the light is avoided (Fig. 2). Because sapphire is not conductive, electrodes for both *n*-type and *p*-type regions must be made on the GaN side. Absorption by the substrate is eliminated by using either semiconductor light reflectors or transparent substrates. In addition, attempts to increase the angle of the cone of emission by growing thick surface layers with small refractive indices have been quite successful. Blue and blue-green InGaN LEDs take advantage of the transparent nature of the sapphire substrates on which they are grown and the high refractive index of InGaN. The LEDs also form regions similar to quantum wells that confine electrons and holes to a small volume. Similar to donor- and acceptor-type impurities, which capture electrons and holes for radiative recombination, these regions can cause an increase in the number of electron-hold interactions, leading to more efficient recombinations.

The combination of high doping on both the *n* and *p* sides and breakthroughs in making low-resistance metal-semiconductor ohmic contacts have reduced the resistive losses so much that they do not represent any major obstacle to commercial implementation. To maximize external quantum efficiency, designers like to dope both sides of the *pn* junction heavily to push the absorption edge to higher energies and also to reduce the series resistances in an effort to increase the power conversion efficiency. Other approaches such as layers with larger band gaps along with heavy doping are more attractive because they avoid absorption tails. To date, commercial LEDs emitting in the red (650 to 660 nm) have the highest conversion efficiencies at 16%, with lasers exhibiting figures as high as 75%. The high-brightness semiconductor LEDs available commercially are based primarily on III-V semiconductors with direct band gaps, such as AlGaAs, InGaAlP, and InGaN (Table 1). In the laboratory, ZnTeSe LEDs emitting in the green and even in the blue have also been achieved (*21*). The lifetime for the green ZnSe LEDs is on the order of 1000 hours. Using a growth technique called seeded physical vapor transport, the scientists at Eagle-Packer have grown large, high-quality ZnSe crystals for substrates with a prospect of building brighter blue ZnSe LEDs. The wavelength of emission of presently available LEDs varies between 450 and 700 nm (laboratory LEDs based on GaN emitting at about 370 nm are available). The luminous intensity (*22*) of these LEDs is in the range of 0.4 to 20 lm/W, depending on the wavelength and the semiconductor used, which is suitable for indicator lamps and numerical readouts.

The external quantum efficiency of an LED equals the internal quantum efficiency multiplied by its extraction efficiency. Because of absorption losses, reflections at the junctions, and total internal reflection at emission angles, which are about 25° for epoxy-encapsulated diodes, the external quantum efficiency is commonly as low as 4% (as was found in the Nichia blue LED) if the active layer is thin. Extraction efficiency, which measures the extraction of photons from an LED's semiconductor chip, is normally much less than unity.

GaN and Its Alloys for Blue and Blue-Green LEDs

An excellent class of semiconductor candidates having the large band gaps necessary to produce visible light on the blue end of the spectrum is GaN and its alloys with InN and AlN. Values of band gap versus lattice constant, the latter being a measure of the proximity of the nearest atoms, for the nitrides in question and various substrate materials are shown in Fig. 3. These large–band gap semiconductors, researched and coveted for the past quarter of a century, are the sources of much current enthusiasm.

The band edge emission in GaN is at 365 nm, which is in the ultraviolet. In order to red-shift it, researchers have used impurity-assisted transitions and addition of InN to GaN, forming the alloy InGaN. The fervent quest for blue light sources and the resilience on the part of nitride researchers finally culminated in the attainment of bright blue and blue-green LEDs. Considerable effort was expended to understand the properties of these materials, leading to the breakthroughs outlined earlier. Studies directed toward high-quality single-crystal growth of films also resulted in remarkable success, and applications of GaN and its alloys started showing encouraging signs of transforming many facets of optoelectronic engineering and technology (*23*).

Bright blue and blue-green LEDs based on the InGaN-AlGaN double heterojunction structures are now available from Nichia Chemical Industries of Japan. In addition, blue LEDs, also based on the InGaN system, are also available from Toyota Gosei. The spectral responses of the Nichia blue and blue-green LEDs at an injection level of 30 mA are shown in Fig. 4. Although the spectrum for both devices is wide, the peak response is at 450 and 500 nm for the blue and blue-green LEDs, respectively. This is due to reliance on the Zn impurity transition for red-shifting the wavelength from the band edge emission of $In_{0.1}Ga_{0.9}N$. For the blue device, the band edge emission would be below 400 nm, which is not considered blue. Increased InN mole fraction in GaN would also red-shift it to 450 nm, but at the expense of introducing additional structural defects because InGaN is not lattice matched to GaN. Lattice-mismatched films can be grown up to a certain thickness for a given composition. The larger the composition, the smaller the critical thickness. The smaller the thickness, the smaller the output power. Considerable debate has ensued, and there is much effort aimed at optimization, and in this case, a 50-nm InGaN was deemed optimum.

The blue-green diode, intended for traffic lights, produces an optical power of about 1 mW at 30 mA, corresponding to a luminous intensity of about 2 cd with an associated external quantum efficiency of 1.4% (Fig. 5). At lower injection levels, the efficiency increases to 1.5%. The peak emission wavelength is 500 nm with a full width at half maximum of about 80 nm at an injection level of 20 mA. An advantage of the InGaN-AlGaN double heterojunction LED over the others is that in this LED, except for the InGaN layer, all of the layers and the substrate are transparent. As mentioned earlier, the substrate would thus not absorb the light incident downward on it. Rather it will reflect the light, providing an increase in the extraction efficiency of the LED.

The external quantum efficiency and total output power of a Nichia blue LED is shown in Fig. 6. The Nichia LED produces 4.5 mW at a forward current of 40 mA. This compares with 90 μW reported for the SiC LEDs produced by Cree Research emitting at 470 nm. In addition, the blue InGaN LED exhibits an external quantum efficiency of about 4% at a power level of 4.5 mW, as compared to a figure that is roughly two orders of magnitude smaller for SiC LEDs. In photometric terminologies, the blue-green LED produces, assuming a monochromatic source at 500 nm, luminous fluxes of 105 and 372 mlm at forward currents of 10 and 40 mA, respectively. A luminous efficacy of 300 lm/W was used for the conversion. The performance of the same (that is, the blue-green LED) is 3.2 and 2.44 lm/W at 10 and 40 mA, respectively. For the blue LED, the luminous flux at 10 and 40 mA is 37.5 and 112 mlm, again assuming a monochromatic source at 450 nm, if a luminous efficacy of 25 lm/W is used. Because the spectral response of the blue LED is wide and the eye response is very wavelength dependent, a convolution must be used to get the accurate luminous flux figures, which will be larger than that reported above. If this correction is made, the luminous performance efficiency at 10 mA of injection current is measured to be 3.6 lm/W as shown in Table 1. This is obtained by dividing the luminous flux at that particular injection current by the electrical power that generated it. The power conversion efficiencies are about 1% and 4.5% at 10 mA for blue-green and blue LEDs.

Nitrides have also attracted attention in the field of digital information storage. Unlike display and lighting applications, digital information storage and reading require coherent light sources, namely lasers. Generally, LEDs are precursory to semiconductor lasers. The output of these coherent light sources can be focused to a diffraction-

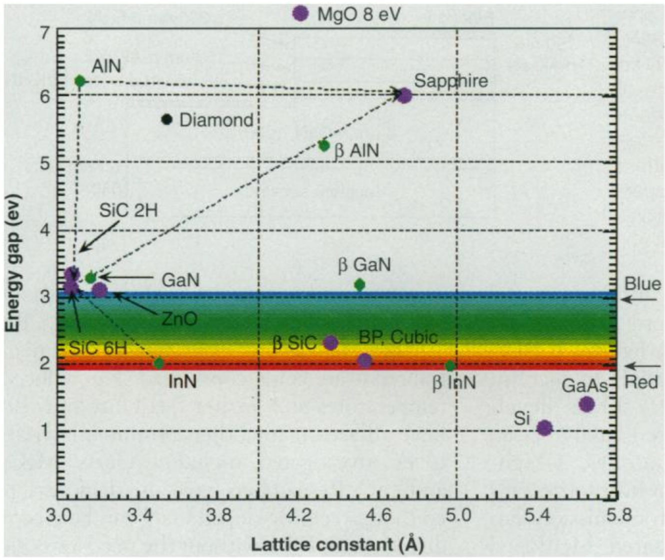

Fig. 3. Energy gap versus lattice spacing for wurtzite and cubic nitrides and some of the substrates on which epitaxial growth have been commonly accomplished. The color bar is not representative of the CIE diagram.

Table 1. Performance of red through blue LEDs.

LED type	Emission wavelength (nm)	Color	Structure*	Conversion efficiency (%)	Performance (lm/W)
GaP:Zn,O	700	Red			0.4
AlGaAs	650	Red	DH–Trans. sub.	16	8
AlInGaP	620	Orange	DH	6	20
InGaAlP	585	Yellow	DH	5	20
InGaAlP	570	Yellow-green	DH	1	6†
GaP	555	Green	HJ	0.1	0.6
ZnTeSe	512		DH	3	13†
InGaN	500	Blue-green	DH	1	
SiC	470		HJ	0.03 to 0.04	0.04
InGaN	450		DH	4.5	3.6

*DH, double heterojunction; Trans. sub., transparent substrate; and HJ, single heterojunction. †Laboratory performance. Laboratory models of InGaAlP LEDs emitting at 600 nm with transparent substrates exhibit a performance of 40 lm/W.

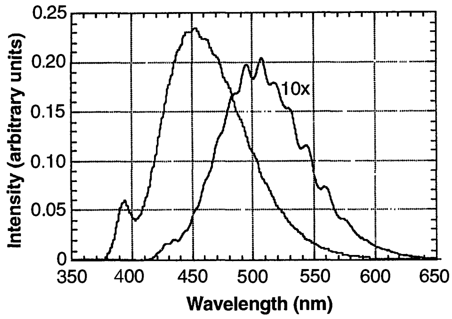

Fig. 4. Light output spectra obtained at 30 mA for a blue and a blue-green Nichia GaN *pn*-junction InGaN double heterojunction LED. The response of the blue-green LED is amplified 10 times.

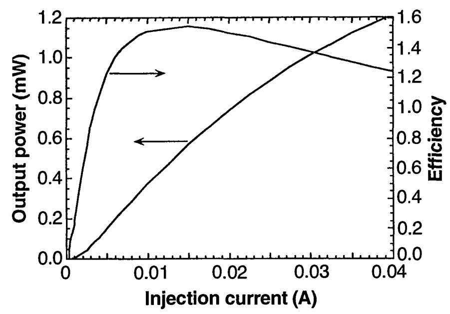

Fig. 5. The output power and the external quantum efficiency versus the injection current in a Nichia InGaN blue-green double heterojunction LED under continuous-wave conditions up to 40 mA.

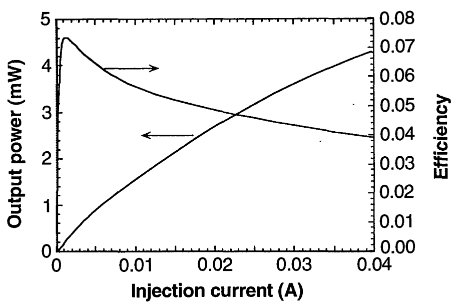

Fig. 6. The output power and the external quantum efficiency versus the injection current in a Nichia InGaN blue double heterojunction LED under continuous-wave conditions up to 40 mA.

limited spot, permitting an optical system in which bits of information can be recorded and read with ease and uncommon accuracy. As the wavelength of the light gets shorter, the focal diameter gets smaller. Significant gains in recording density can be achieved by using GaN-based lasers that operate at shorter wavelengths. The nitride-based materials system, when adapted to semiconductor lasers in blue and ultraviolet wavelengths, offers increased data storage density possibly in excess of 1 gigabyte per square centimeter. These prospects lured numerous corporations across the globe to rush to build lasers for an affordable compact digital information storage system. Present approaches rely on wavelength doubling of high-power red lasers. They are bulky and expensive, and thus, compact coherent sources emitting at the wavelength of interest are preferable. Although II-VI compound semiconductors, such as zinc selenide ($E_g = 2.67$ eV) and its pseudomorphic ternary and lattice-matched quaternary alloys, have led to the demonstration of 490-nm diode lasers (*24*), they suffer from several weaknesses. For example, ZnSe has low thermal conductivity and thus poor thermal stability, large ohmic contact resistances, and a low damage threshold, making lifetimes of these devices very short. Moreover, shorter wavelengths in the ultraviolet, which are outside the reach of present ZnSe-based devices, would be better for higher density.

Conclusions

Researchers have made great strides in recent years in fabricating LEDs from GaN. The use of nitrides paved the way for the attainment of blue emitters having longevity and luminous performance acceptable for outdoor display applications. These developments are in part possible because of the innate bond strength of this material system in that the generation and mobility of killer defects during operation is low.

In order to obtain reliable lasers for digital recording applications, researchers must reduce the structural defect concentration, which currently runs in the 10^8 to 10^{11} cm^{-2} range, by innovative defect control coupled with appropriate advances in substrate development and deposition. The blue emission of Nichia LEDs has a spectral width of several hundred millielectron volts. These LEDs take advantage of the deep, acceptor-like states of Mg or Zn (or both). Whether this deep-level nature will suit the diode laser, which requires population inversion for gain, should be addressed. Although hydrogen was identified as the critical compensating agent for the growth of *p*-GaN, the role of the hydrogen-free environment has not yet been fully established. The problems with *p*-type doping, particularly using the MBE technique, are still far from being completely resolved.

All these and other issues to the aforementioned problems are being vigorously explored. In a few short years time, it is expected that many advantages offered by nitrides will come to fruition. In short, the light emitters based on GaN and its allied alloys are extremely bright and so is the future for this ubiquitous material system.

REFERENCES AND NOTES

1. Brightness is a subjective term used to describe the perception of the human eye, such as very dim on the one hand and blinding on the other.
2. Luminous flux: power of visible light in photometric terms.
3. M. G. Craford, *IEEE Circuits Devices Mag.* **8**, 24 (1992); M. G. Craford and F. M. Steranka, in *Encyclopedia of Applied Physics*, G. Trigg, Ed. (VCH Publishers, New York, 1994), vol. 8, p. 485; K. Werner, *IEEE Spectrum* **31**, 30 (1994).
4. M. E. Hoenecke, R. J. Bula, T. W. Tibbitts, *HortScience* **27**, 427 (1992).
5. Luminance is defined as the luminous intensity per unit area projected in a certain direction. It has SI units candelas per square meter.
6. R. Englemann, private communication.
7. N. Nakamura, T. Mukai, M. Seno, *Appl. Phys. Lett.* **64**, 1687 (1994).
8. *Optoelectronics/Fiber-Optics Applications Manual* (McGraw-Hill, New York, 1990), sect. 7.
9. T. V. Higgins, *Laser Focus World* **30**, 62 (1994), for photo research CIE 1976 chromaticity diagram.
10. H. P. Maruska and J. J. Tietjen, *Appl. Phys. Lett.* **15**, 327 (1969).
11. M. Hashimoto, H. Amano, N. Sawaki, I. Akasaki, *J. Cryst. Growth* **68**, 163 (1984).
12. M. Mizuta, S. Fujieda, Y. Matsumoto, T. Kawamura, *Jpn. J. Appl. Phys.* **25**, L945 (1986); M. J. Paisley, Z. Sitar, J. B. Posthill, R. F. Davis, *J. Vac. Sci. Technol. A* **7**, 701 (1989); S. Strite *et al.*, *J. Vac. Sci. Technol. B* **9**, 1924 (1991); T. Lei *et al.*, *Appl. Phys. Lett.* **59**, 944 (1991).
13. T. Sasaki and T. Matsuoka, *J. Appl. Phys.* **64**, 4531 (1988); M. A. Khan *et al.*, *Appl. Phys. Lett.* **58**, 526 (1991).
14. S. Nakamura, Y. Harada, M. Seno, *Appl. Phys. Lett.* **58**, 2021 (1991).
15. J. I. Pankove, E. A. Miller, J. E. Berkeyheiser, *RCA Rev.* **32**, 383 (1971).
16. H. Amano, M. Kito, K. Hiramatsu, I. Akasaki, *Jpn. J. Appl. Phys.* **28**, L2112 (1989).
17. S. Nakamura, N. Iwasa, M. Seno, T. Mukai, *ibid.* **31**, 1258 (1992).
18. J. A. Van Vechten, J. D. Zook, R. D. Horning, B. Goldenberg, *ibid.*, p. 3662.
19. I. Akasaki and H. Amano, *Mater. Res. Soc. Symp. Proc.* **242**, 383 (1991).
20. R. J. Molnar, T. Lei, T. D. Moustakas, *Mater. Res. Soc. Symp. Proc.* **281**, 753 (1993); M. E. Lin, G. Xue, G. L. Zhou, J. E. Greene, H. Morkoç, *Appl. Phys. Lett.* **63**, 932 (1993); C. Wang and R. Davis, *ibid.*, p. 990.
21. D. B. Eason *et al.*, *Electron. Lett.*, in press.
22. Luminous intensity is defined as the luminous flux per solid angle emitted from a point. The units are lumens per steradian, or candelas (cd).
23. R. F. Davis, *Proc. IEEE* **79**, 702 (1991); S. Strite and H. Morkoç, *J. Vac. Sci. Technol. B* **10**, 1237 (1992); S. Strite, M. E. Lin, H. Morkoç, *Thin Solid Films* **231**, 197 (1993); H. Morkoç *et al.*, *J. Appl. Phys.* **76**, 1363 (1994); H. Morkoç in *CRC Handbook on Optoelectronics*, M. Gupta, Ed. (CRC Press, Boca Raton, FL, in press).
24. A. V. Nurmikko and R. L. Gunshor, *IEEE J. Quantum Electron.* **30**, 619 (1994).

25. Funding from the U.S. Office of Naval Research and U.S. Air Force Office of Scientific Research is gratefully acknowledged. Special appreciation is owed to I. Akasaki, S. Nakamura, and B. Goldenberg for sharing many of their thoughts, data, and devices, and to G. L. Witt and M. Yoder for their support and encouragement. The authors are grateful to J. Schetzina and R. Englemann for useful discussions and providing preprints of their work, B. Sverdlov for measuring the Nichia LEDs, and K. Suzue and D. Li for careful readings of the manuscript.